

Precise temporal localisation of M/EEG effects with Bayesian generalised additive multilevel models

Ladislav Nalborczyk¹ and Paul Bürkner²

¹Aix Marseille Univ, CNRS, LPL

²TU Dortmund University, Department of Statistics

Abstract

Time-resolved electrophysiological measurements such as those obtained through magneto- or electro-encephalography (M/EEG) offer a unique window into the neural activity underlying cognitive processes. Researchers are often interested in determining whether and when these signals differ across experimental conditions or participant groups. The conventional approach involves mass-univariate statistical testing across time, followed by corrections for multiple comparisons (e.g., FDR, FWER) or cluster-based inference. While effective for controlling error rates, cluster-based methods come with a significant limitation: they shift the focus of inference from individual time points to clusters, making it difficult to draw precise conclusions about the onset or offset of observed effects. Here, we introduce a *model-based* approach for analysing M/EEG timeseries such as event-related potentials (ERPs) or decoding performance over time. Our method leverages Bayesian generalised additive multilevel models (GAMMs), providing posterior probabilities that an effect is above zero (or above chance) at each time point, while naturally accounting for temporal dependencies and between-subject variability. Using both simulated and actual M/EEG datasets, we demonstrate that this approach substantially outperforms conventional methods in estimating the onset and offset of neural effects, yielding more precise and reliable results. We also provide an R package implementing the method and show how it can be seamlessly integrated into M/EEG analysis pipelines using MNE-Python.

Keywords: EEG, MEG, generalised additive models, mixed-effects models, multilevel models, Bayesian statistics, brms

Table of contents

Introduction	3
Introduction	3
Problem statement	3

Ladislav Nalborczyk  <https://orcid.org/0000-0002-7419-9855>

Paul Bürkner  <https://orcid.org/0000-0001-5765-8995>

The authors have no conflicts of interest to disclose.

Correspondence concerning this article should be addressed to Ladislav Nalborczyk, Aix Marseille Univ, CNRS, LPL, 5 avenue Pasteur, 13100 Aix-en-Provence, France, email: ladislav.nalborczyk@cnrs.fr

12	Related work	3
13	Bayesian regression modelling	3
14	Generalised additive models	3
15	Bayesian generalised additive multilevel models	4
16	Objectives	4
17	Methods	5
18	M/EEG data simulation	5
19	Model fitting	5
20	Multilevel modelling using summary statistics	7
21	Error properties of the proposed approach	8
22	Comparing the identified onsets/offsets to other approaches	9
23	Simulation study	10
24	Application to actual MEG data	10
25	Results	12
26	Simulation study (bias and variance)	12
27	Application to actual MEG data (reliability)	13
28	Discussion	15
29	Summary of the proposed approach	15
30	Limitations and future directions	15
31	Data and code availability	16
32	Packages	16
33	Acknowledgements	16
34	References	17
35	Application to 2D time-resolved decoding results (cross-temporal generalisation)	22
36	Alternative to GAMs: Approximate Gaussian Process regression	25
37	How to choose the GAM basis dimension?	26
38	Integration with MNE-Python	27

Precise temporal localisation of M/EEG effects with Bayesian generalised additive multilevel models

Introduction

Understanding the temporal dynamics of cognitive processes requires methods that can capture fast-changing neural activity with high temporal resolution. Magnetoencephalography (MEG) and electroencephalography (EEG) are two such methods, widely used in cognitive neuroscience for their ability to track brain activity at the millisecond scale. These techniques provide rich time series data that reflect how neural responses unfold in response to stimuli or tasks. A central goal in many M/EEG studies is to determine whether and when neural responses differ across experimental conditions or participant groups.

Here are some useful references to be discussed ([Combrisson & Jerbi, 2015](#); [Ehinger & Dimigen, 2019](#); [Frossard & Renaud, 2021, 2022](#); [Gramfort, 2013](#); [Hayasaka, 2003](#); [Luck & Gaspelin, 2017](#); [Maris & Oostenveld, 2007](#); [Pernet et al., 2015](#))... See also [Maris \(2011\)](#) and [Rosenblatt et al. \(2018\)](#) (history of cluster-based approaches)... Clusters failures ([Eklund et al., 2016](#))...

Problem statement

Description of cluster-based approaches (see [Sassenhagen & Draschkow, 2019](#))...

However, as pointed by the original authors themselves ([Maris & Oostenveld, 2007](#)), “there is a conflict between this interest in localized effects and our choice for a global null hypothesis: by controlling the FA [false alarm] rate under this global null hypothesis, one cannot quantify the uncertainty in the spatiotemporal localization of the effect” ([Maris & Oostenveld, 2007](#); [Sassenhagen & Draschkow, 2019](#)). In contrast, the proposed approach, based on Bayesian generalised additive multilevel models, allows quantifying the posterior probability of effects being above chance at the level of timesteps, voxels, sensors (etc), while naturally taking into account spatiotemporal dependencies present in M/EEG timeseries.

Related work

Recent example of GLM for EEG ([Fischer & Ullsperger, 2013](#); [Wüllhorst et al., 2025](#))... See also ([Hauk et al., 2006](#); [Rousselet et al., 2008](#))... Example of two-stage regression analysis (i.e., individual-level then group-level, [Dunagan et al., 2024](#))...

See also the rERP framework ([N. J. Smith & Kutas, 2014a, 2014b](#)) and Tremblay & Newman ([2014](#))...

From Dimigen & Ehinger ([2021](#)): Recently, spline regression has been applied to ERPs (e.g., [Hendrix et al., 2017](#); [Kryuchkova et al., 2012](#))... GAMMs for EEG data ([Abugaber et al., 2023](#); [Meulman et al., 2015, 2023](#))...

Disentangling overlapping processes ([Skukies et al., 2024](#); [Skukies & Ehinger, 2021](#))... Weighting single trials ([Pernet, 2022](#))... The LIMO toolbox ([Pernet et al., 2011](#))...

Recently, Teichmann ([2022](#)) provided a detailed tutorial on using Bayes factors (BFs) to analyse the 1D or 2D output from MVPA, that is, for testing, at every timestep, whether decoding performance is above chance level. However, this approach provides timeseries of BFs that ignores temporal dependencies..

Bayesian regression modelling

Short intro/recap about Bayesian (linear and generalised) regression models...

Generalised additive models

See for instance these tutorials ([Sóskuthy, 2017](#); [Winter & Wieling, 2016](#)) or application to phonetic data ([Sóskuthy, 2021](#); [Wieling, 2018](#)) or this introduction ([Baayen & Linke, 2020](#)) or

these reference books (Hastie & Tibshirani, 2017; Wood, 2017a)... application to pupillometry (Rij et al., 2019)... GAMLSS for neuroimaging data (Dinga et al., 2021)... Modelling auto-correlation in GAMMs + EEG example (Baayen et al., 2018)...

In generalised additive models (GAMs), the functional relationship between predictors and response variable is decomposed into a sum of low-dimensional non-parametric functions. A typical GAM has the following form:

$$y_i \sim \text{EF}(\mu_i, \phi)$$

$$g(\mu_i) = \underbrace{\mathbf{A}_i \gamma}_{\text{parametric part}} + \underbrace{\sum_{j=1}^J f_j(x_{ij})}_{\text{non-parametric part}}$$

where $y_i \sim \text{EF}(\mu_i, \phi)$ denotes that the observations y_i are distributed as some member of the exponential family of distributions (e.g., Gaussian, Gamma, Beta, Poisson) with mean μ_i and scale parameter ϕ ; $g(\cdot)$ is the link function, \mathbf{A}_i is the i th row of a known parametric model matrix, γ is a vector of parameters for the parametric terms (to be estimated), f_j is a smooth function of covariate x_j (to be estimated as well). The smooth functions f_j are represented in the model via penalised splines basis expansions of the covariates, that are a weighted sum of K simpler, basis functions:

$$f_j(x_{ij}) = \sum_{k=1}^K \beta_{jk} b_{jk}(x_{ij})$$

where β_{jk} is the weight (coefficient) associated with the k th basis function $b_{jk}(\cdot)$ evaluated at the covariate value x_{ij} for the j th smooth function f_j . To clarify the terminology at this stage: *splines* are functions composed of simpler functions. These simpler functions are basis functions (e.g., a cubic polynomial) and the set of basis functions is a *basis*. Each basis function gets its coefficient and the resultant spline is the sum of these weighted basis functions. Splines coefficients are penalised (usually through the squared of the smooth functions' second derivative) in a way that can be interpreted, in Bayesian terms, as a prior on the "wiggleness" of the function. In other words, more complex (wiggly) basis function are penalised.

Bayesian generalised additive multilevel models

Introduction to multilevel GAMs (E. J. Pedersen et al., 2019)...

Now describe the Bayesian GAMM (Miller, 2025)... Proper inclusion of varying/random effects in the model specification protects against overly wiggly curves (Baayen & Linke, 2020)... Generalising to scale and shape or "distributional GAMs" (Rigby & Stasinopoulos, 2005; Umlauf et al., 2018) and applied to neuroimaging data (Dinga et al., 2021)...

Instead of averaging, obtain the smooth ERP signal from multilevel GAM... less susceptible to outliers (Meulman et al., 2023)...

Objectives

Given the previously reported limitations of conventional methods to precisely identify the onset and offset of M/EEG effects (e.g., ERPs, decoding performance), we aimed to provide a model-based approach for estimating the onset and offset of such effects. To achieve this, we leveraged Bayesian generalised additive multilevel models (BGAMMs) fitted via the **brms** R package and compared the performance of this approach to conventional methods on both simulated and actual M/EEG data.

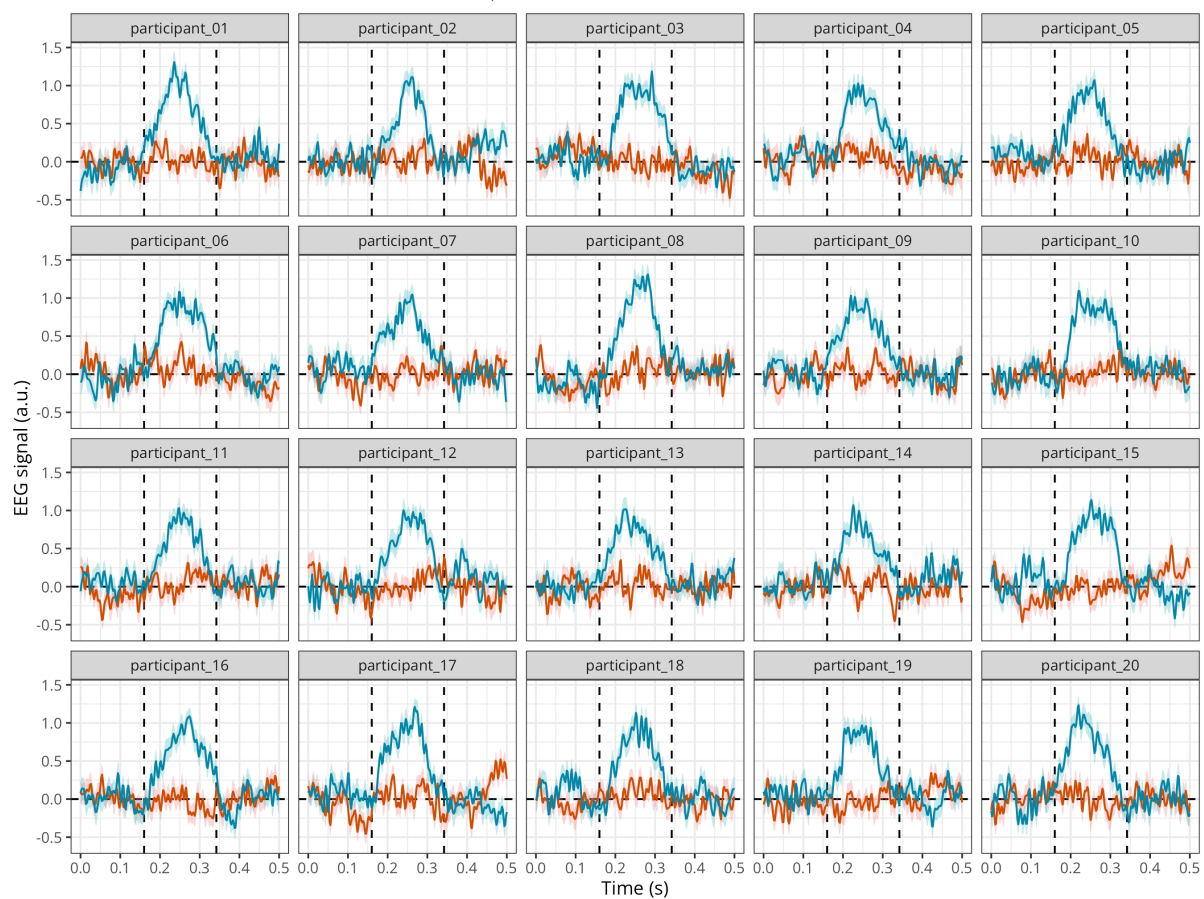
Methods

M/EEG data simulation

Following the approach of Sassenhagen & Draschkow (2019) and Rousselet (2025), we simulated EEG data stemming from two conditions, one with noise only, and the other with noise + signal. As in previous studies, the noise was generated by superimposing 50 sinusoids at different frequencies, following an EEG-like spectrum (see code in the online supplementary materials and details in Yeung et al., 2004). As in Rousselet (2025), the signal was generated from truncated Gaussian with an objective onset at 160 ms, a peak at 250 ms, and an offset at 342 ms. We simulated this signal for 250 timesteps between 0 and 0.5s, akin to a 500 Hz sampling rate. We simulated data for a group of 20 participants with 50 trials per participant and condition (Figure 1).

Figure 1

Mean simulated EEG activity in two conditions with 50 trials each, for a group of 20 participants. The error band represents the mean \pm 1 standard error of the mean.



Model fitting

We then fitted a Bayesian GAM using the `brms` package (Bürkner, 2017, 2018; Nalborczyk et al., 2019). We used the default priors in `brms` (i.e., weakly informative priors). We ran eight Markov Chain Monte-Carlo (MCMC) to approximate the posterior distribution, including each 5000 iterations and a warmup of 2000 iterations, yielding a total of $8 \times (5000 - 2000) = 24000$ posterior samples to use for inference. Posterior convergence was assessed examining trace plots as well as the Gelman–Rubin statistic \hat{R} (Gabry et al., 2019; Gelman et al., 2020). The `brms`

98 package uses the same syntax as the R package `mgcv` v 1.9-1 (Wood, 2017b) for specifying
 99 smooth effects. Figure 2 shows the predictions of this model together with the raw data.

```
# averaging across participants
ppt_df <- raw_df %>%
  group_by(participant, condition, time) %>%
  summarise(eeg = mean(eeg) ) %>%
  ungroup()

# defining a contrast for condition
contrasts(ppt_df$condition) <- c(-0.5, 0.5)

# timing the model fitting
# around 600s for 2000 iterations on 4 chains and 4 cores
# around 190s for 2000 iterations on 4 chains and 4 cores + cmdstanr and 01
# around 440s for 2000 iterations on 4 chains and 4 cores + threading(2), cmdstanr and 01
# library(tictoc)
# tic()

# fitting the GAM
gam <- brm(
  # cubic regression splines with k-1 basis functions
  # eeg ~ condition + s(time, bs = "cr", k = 20, by = condition),
  # thin-plate regression splines with k-1 basis functions
  eeg ~ condition + s(time, bs = "tp", k = 20, by = condition),
  data = ppt_df,
  family = gaussian(),
  warmup = 2000,
  iter = 5000,
  chains = 8,
  cores = 8,
  file = "models/gam.rds"
  #####
  # speeding up the model fitting #
  #####
  # backend = "cmdstanr",
  # threads = threading(2),
  # stan_model_args = list(stanc_options = list("01") )
)

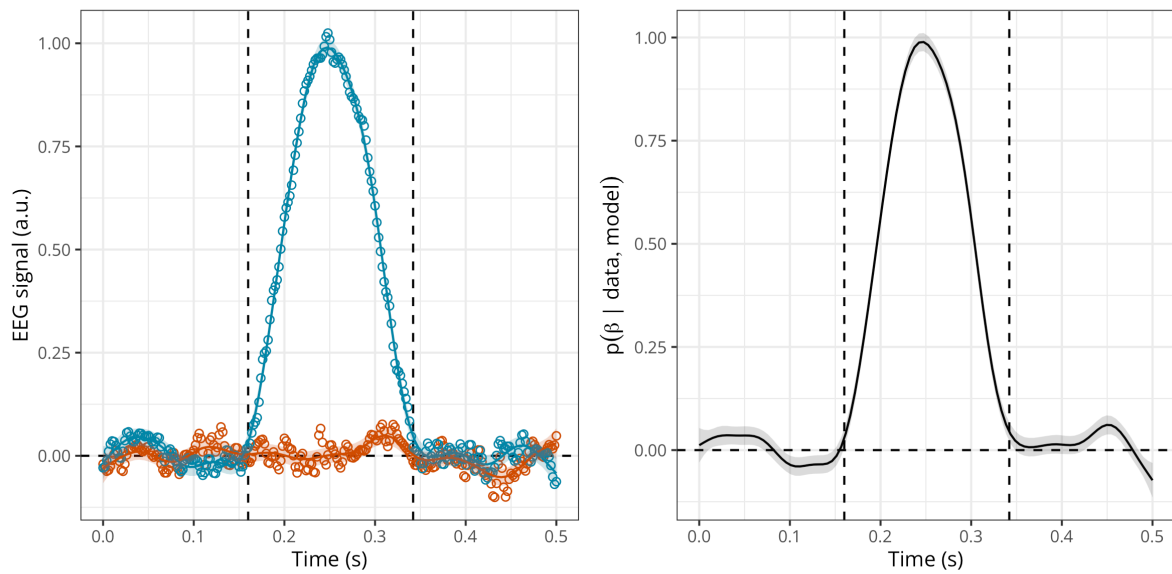
# stop timing
# toc()
```

100 We depict the posterior predictions together with the posterior estimate of the slope for
 101 **condition** at each timestep (Figure 2).

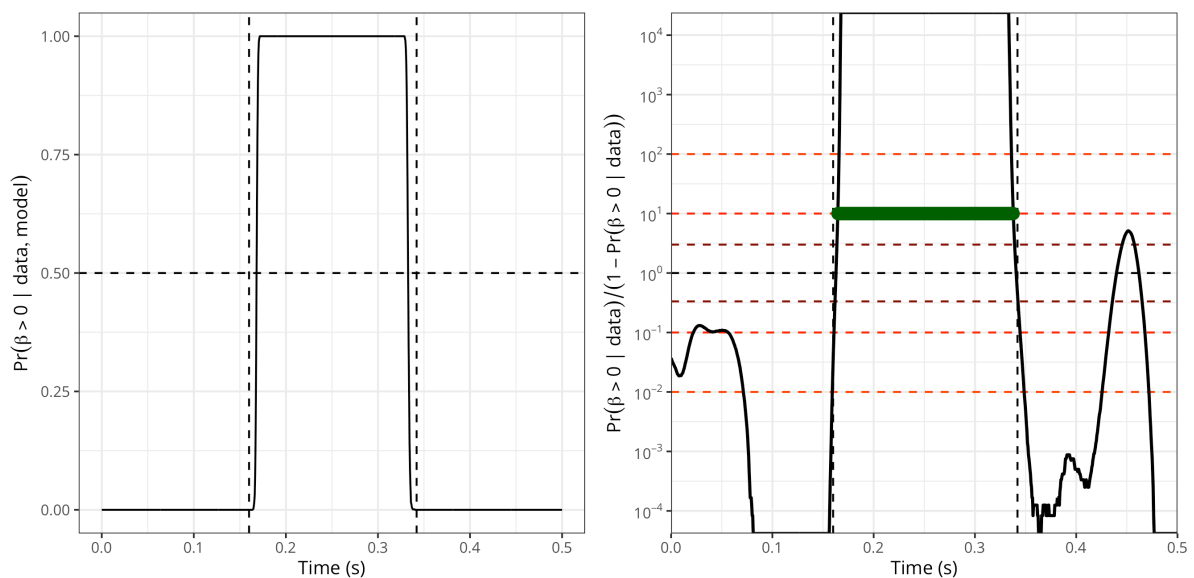
102 We then compute the posterior probability of the slope for **condition** being above 0
 103 (Figure 3, left). We can also express this as the ratio of posterior probabilities (i.e., $p/(1-p)$)
 104 and visualise the timecourse of this ratio superimposed with the conventional thresholds on
 105 evidence ratios (Figure 3, right). A ratio of 10 means that the probability of the difference
 106 being above 0 is 10 times higher than the probability of the difference not being above 0, given
 107 the data, the priors, and other model's assumptions.

Figure 2

Posterior estimate of the EEG activity in each condition (left) and posterior estimate of the difference in EEG activity (right) according to the GAM.

**Figure 3**

Left: Posterior probability of the EEG difference (slope) being above 0 according to the GAM. Right: Ratio of posterior probability according to the GAM (on a log10 scale). Timesteps above threshold (10) are highlighted in green.



108 Multilevel modelling using summary statistics

109 The previous model only included constant (fixed) effects, thus not properly accounting
 110 for between-participant variability. We next fit a multilevel version of the GAM. Although it
 111 is possible to fit a GAMM at the single-trial level, we present a resource-efficient version of the
 112 model that is fitted directly on the by-participant summary statistics (mean and SD), similar
 113 to what is done in meta-analysis.

```

# averaging across participants
summary_df <- raw_df %>%
  summarise(
    eeg_mean = mean(eeg),
    eeg_sd = sd(eeg),
    .by = c(participant, condition, time)
  )

# defining a contrast for condition
contrasts(summary_df$condition) <- c(-0.5, 0.5)

# fitting the GAM
meta_gam <- brm(
  # using by-participant SD of ERPs across trials
  eeg_mean | se(eeg_sd) ~
    condition + s(time, bs = "cr", k = 20, by = condition) +
    (1 | participant),
  data = summary_df,
  family = gaussian(),
  warmup = 2000,
  iter = 5000,
  chains = 8,
  cores = 8,
  file = "models/meta_gam.rds"
)

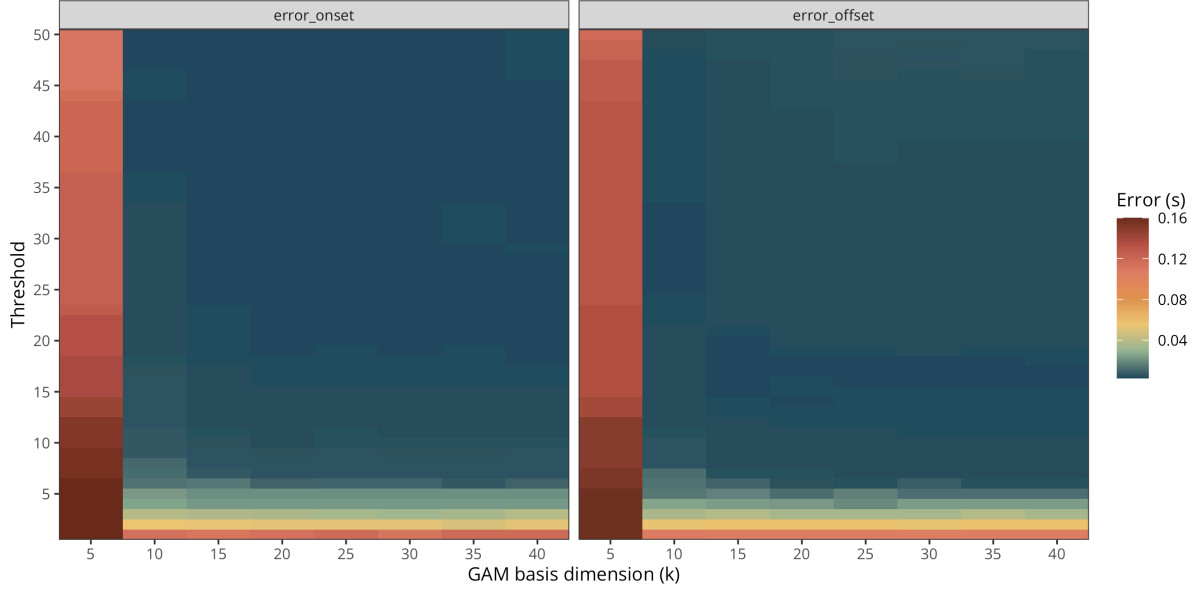
```

114 Error properties of the proposed approach

115 We then compute the difference between the true and estimated onset/offset of the EEG
 116 difference according to various k (GAM basis dimension) and `threshold` values. Remember
 117 that the EEG signal was generated from a truncated Gaussian with an objective onset at 160
 118 ms, a maximum at 250 ms, and an offset at 342 ms. Figure 4 shows that the multilevel GAM
 119 can *almost exactly* recover the true onset and offset values, given some reasonable choice of k
 120 and `threshold` values (e.g., a threshold of 20). We provide more detailed recommendations on
 121 how to set k in Section C.

Figure 4

Average estimation error for the onset (left) and offset (right) according to various basis dimension and threshold values (according to the multilevel GAM).

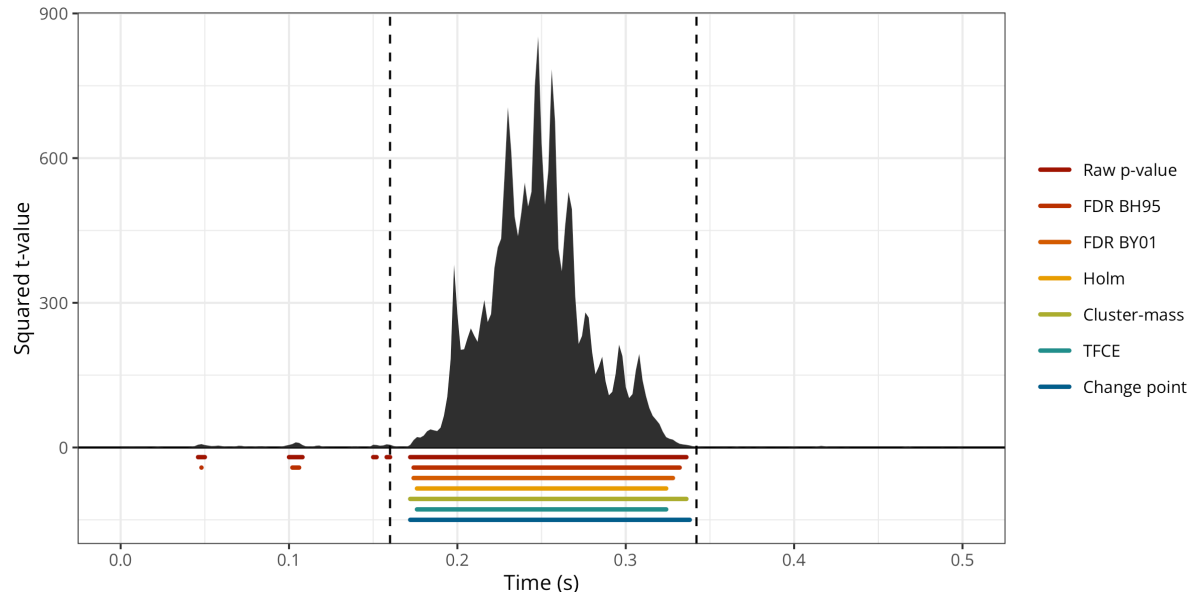


Comparing the identified onsets/offsets to other approaches

We then compared the ability of the GAMM to correctly estimate the onset and offset of the ERP difference to other widely-used methods. First, we conducted mass-univariate t-tests (thus treating each timestep independently) and identified the onset and offset of the ERP difference as the first and last values crossing an arbitrary significance threshold ($\alpha = 0.05$). We then followed the same approach but after applying different forms of multiplicity correction to the p-values. We compared two methods that control the false discovery rate (FDR) (i.e., BH95, [Benjamini & Hochberg, 1995](#); and BY01, [Benjamini & Yekutieli, 2001](#)), one method that controls the family-wise error rate (FWER) (i.e., Holm–Bonferroni method, [Holm, 1979](#)), and two cluster-based permutation methods (permutation with a single cluster-forming threshold and threshold-free cluster enhancement, TFCE, [S. Smith & Nichols, 2009](#)). The BH95, BY01, and Holm corrections were applied to the p-values using the `p.adjust()` function in R. The cluster-based inference was implemented using a cluster-sum statistic of squared t-values, as implemented in MNE-Python ([Gramfort, 2013](#)), called via the R package `reticulate` v 1.42.0 ([Ushey et al., 2024](#)). We also compared these estimates to the onset and offset as estimated using the binary segmentation algorithm, as implemented in the R package `changepoint` v 2.3 ([Killick et al., 2022](#)), and applied directly to the squared t-values (as in [Rousselet, 2025](#)). Figure 5 illustrates the onsets and offsets estimated by each method on a single simulated dataset and shows that all methods over-estimate the true onset and under-estimate the true offset.

Figure 5

Exemplary timecourse of squared t -values with true onset and offset (vertical black dashed lines) and onsets/offsets identified using the raw p -values, the corrected p -values (BH95, BY01, Holm), the cluster-based methods (Cluster-mass, TFCE), or using the binary segmentation method (Change point).



Simulation study

The various methods were compared using the median error (i.e., true-estimated) and variance of onset/offset estimates computed on 10.000 simulated datasets.

Application to actual MEG data

To provide a more exhaustive assessment of these methods, we also evaluated the performance of the proposed approach on actual MEG data (decoding results from [Nalborczyk et al., in preparation](#)). In this study, we conducted time-resolved multivariate pattern analysis (MVPA, also known as decoding) of MEG data during reading tasks. As a result, we obtain a timecourse of decoding performance (ROC AUC), bounded between 0 and 1, for each participant (for a total of 32 participants). Next, we want to *test* whether the group-level average decoding accuracy is above chance (i.e., 0.5) at each timestep (Figure 6). To achieve this, we fitted a similar GAM as discussed previously, but we replaced the Normal likelihood function by a Beta one to account for the bounded nature of AUC values (between 0 and 1) (for a tutorial on Beta regression, see [Coretta & Bürkner, 2025](#)).

Note that although we chose a basis dimension of $k = 50$, which seems appropriate for the present data, this choice should be adapted according to the properties of the modelled data (e.g., signal-to-noise ratio, prior low-pass filtering, sampling rate, etc) and should be assessed by the usual model checking tools (e.g., posterior predictive checks, see also Section C). To better distinguish signal from noise, we also defined a region of practical equivalence (ROPE, [Kruschke & Liddell, 2017](#)), defined as the chance level plus the standard deviation of the (group-level average) decoding performance during the baseline period.

```
# fitting the Beta GAM
meg_decoding_gam <- brm(
  auc ~ s(time, bs = "cr", k = 50),
```

```

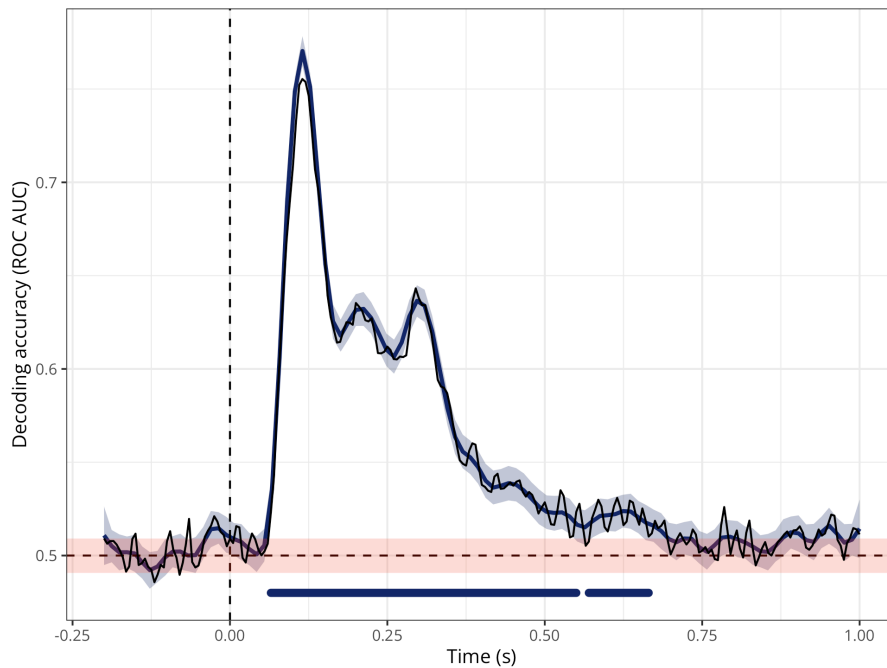
data = decoding_df,
family = Beta(),
warmup = 2000,
iter = 5000,
chains = 4,
cores = 4
)

```

162 We assessed the reliability of the proposed approach using a form of permutation-based
163 split-half reliability (as for instance in [Rosenblatt et al., 2018](#)), which consisted of the following
164 steps. First, we created 1000 split halves of the data (i.e., with half the participants in the
165 original data, that is, 16 participants). For each split, we estimated the onset/offset using all
166 methods described previously. Third, we summarised the distribution of onset/offset estimates
167 using the median “error” (i.e., difference between the split estimate and the estimate obtained
168 using the full dataset) and the variance across splits. This approach allows assessing how similar
169 the estimate of each half split is to the full dataset (thus acting as a proxy for the population)
170 and how variable the estimates are (across split halves).

Figure 6

Group-level average decoding performance ($N=32$) superimposed with the GAM predictions (in blue) and the region of practical equivalence (ROPE, in orange) computed from the baseline period. The blue horizontal markers indicate the timesteps at which the posterior probability ratio exceeds 20.



Results

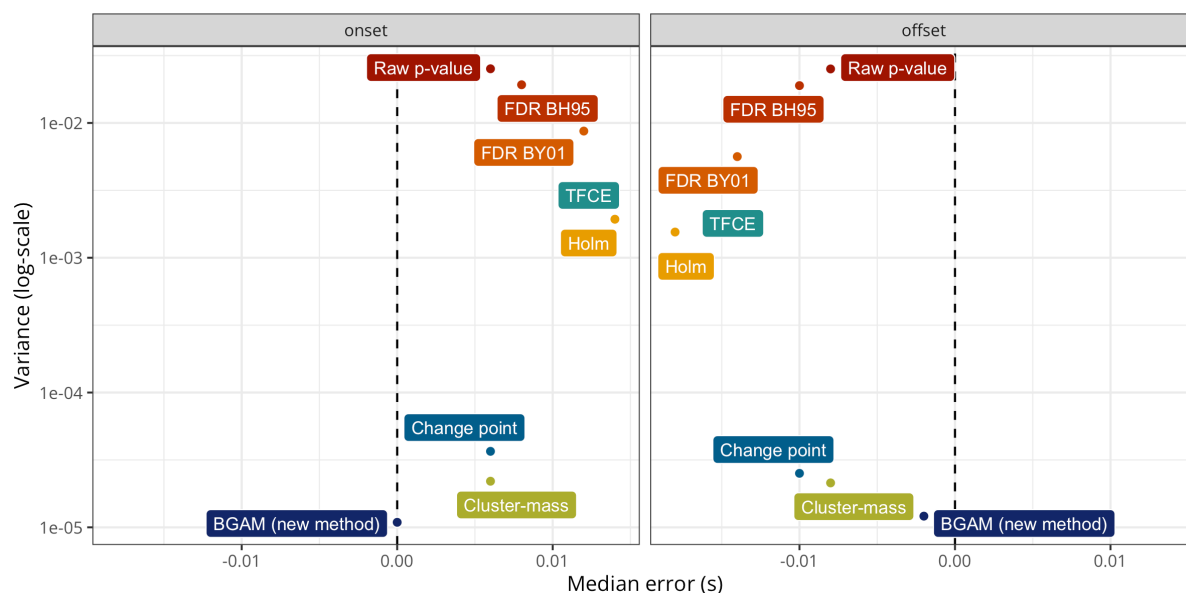
This section is divided in two parts. First, we present the results from the simulation study, assessing the bias and variance of each method when applied to simulated data in which the ground truth is known. Second, we present the results obtained when applying the different methods to actual MEG data (decoding performance through time), assessing the reliability of the estimates provided by each method.

Simulation study (bias and variance)

Figure 7 shows a summary of the simulation results, revealing that the proposed approach (BGAM) has the lowest median error and variance for both the onset and offset estimates. The **Cluster-mass**, **Holm**, and **Change point** also have good performance, but surprisingly, the **TFCE** method has relatively bad performance for estimating the effect offset. Unsurprisingly, the **Raw p-value**, **FDR BH95**, and **FDR BY01** methods show the worst performance.

Figure 7

Median error and variance of onset and offset estimates for each method. The vertical dashed line represents an unbiased estimate of the true onset/offset. Variance is plotted on a log10 scale for visual purposes.



Application to actual MEG data (reliability)

Figure 8 shows the group-level average decoding performance through time with onset and offset estimates for each method. Overall, this figure shows that both the **Raw p-value** and **FDR BH95** methods are extremely lenient, considering that the decoding performance is above chance before the onset of the stimulus (false positive) and until the end of the trial. The **Change point** and **Cluster mass** methods seem the most conservative methods, identifying a time window from approximately +60ms to +500ms. The **Holm**, **TFCE**, and **BGAM** methods produce similar estimates of onset and offset, ranging from approximately +60ms to +650ms, although the **BGAM** method seems to result in fewer clusters.¹

Figure 8

Group-level average decoding performance through time with onset and offset estimates for each method (data from [Nalborczyk et al., in preparation](#)).

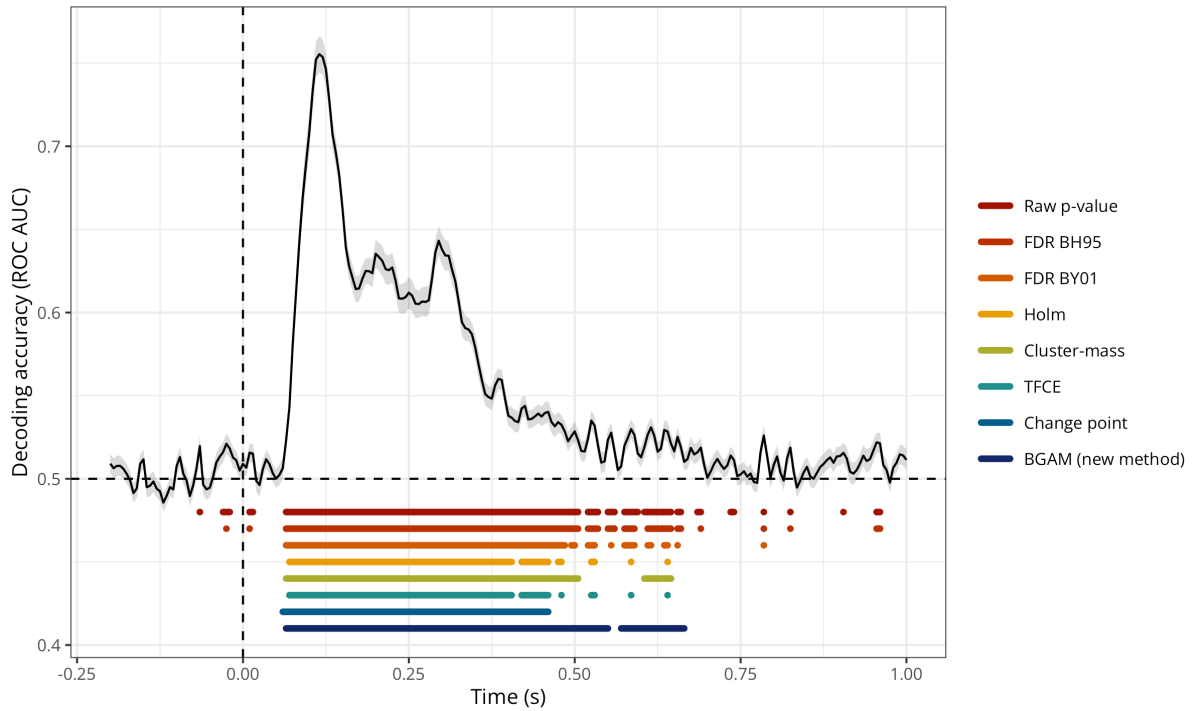


Figure 9 shows the median difference between the onset and offset estimates from each data split and the onset and offset estimates from the full dataset (x-axis) along with the variance of its onset and offset estimates across data splits (error bar). This figure reveals that the **BGAM onset and offset** estimates on each split are the closest to the estimates from the full dataset on average (0ms difference for the onset estimate and 5ms difference for the offset estimate). The **Raw p-value** method has similar performance, but given the aberrant estimates it produces (cf. Figure 8), the fact that it is consistent between data splits and the full dataset is not convincing on its own. The **Change point** method also has a very good performance (i.e., very low difference between split estimates and full estimates), but produces too short cluster of significant decoding performance (cf. Figure 8).² Overall, the figure reveals that for all other methods, split datasets produce later onset estimates and earlier offset estimates (as compared to the estimates from the model fitted on the full dataset). These results highlight that the

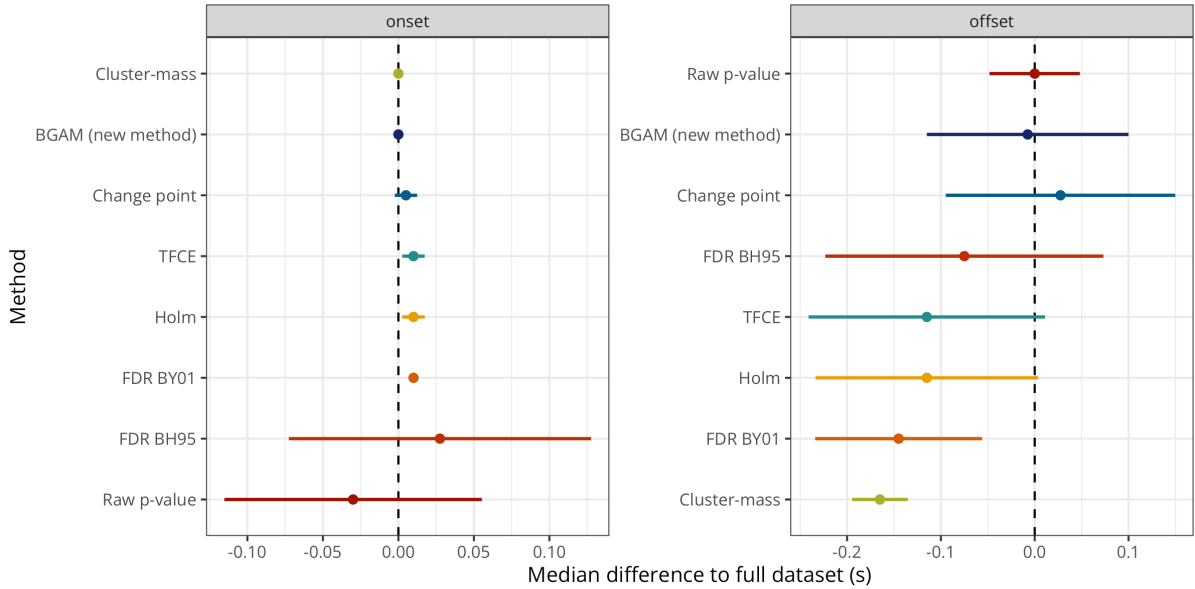
¹It should be noted that although each method can produce several “clusters” of “significant” timesteps, we only considered the first (onset) and last (offset) timesteps identified by each method to compute the estimation error.

²As in Rousselet (2025), we fixed the number of expected change points to two in the binary segmentation algorithm, thus producing always one cluster.

204 results of any method should be assessed using both i) good asymptotic properties on simulated
205 data, ii) sensible identified clusters in actual data, and iii) reliable/stable estimates on actual
206 data.

Figure 9

Median error and median absolute deviation of the error for the onset (left) and offset (right) estimates according to each method. Methods are ordered from lowest (top) to highest (bottom) median absolute error (separately for the onset and offset estimates).



Discussion

Summary of the proposed approach

Overall, before concluding on the onset/offset of effect based on the model, we need to ensure that the model provides a faithful description of the data-generating process (e.g., via posterior predictive checks etc)...

Limitations and future directions

As in previous simulation work (e.g., [Rousselet et al., 2008](#); [Sassenhagen & Draschkow, 2019](#)), the present simulation results depend on various choices such as the specific cluster-forming algorithm and threshold, signal-to-noise ratio, negative impact of preprocessing steps (e.g., low-pass filter) on temporal resolution... note however, that the same caveats apply to all methods...

The error properties depend on the threshold parameter, a value of 10 or 20 seems to be a reasonable default, but the optimal threshold parameter can be adjusted using split-half reliability assessment...

Can be applied to any 1D timeseries (e.g., pupillometry, electromyography)... Extending the approach to spatiotemporal data (i.e., time + sensors)...

We kept the exemplary models simple, but can be extended by adding varying/random effects (intercept and slope) for item (e.g., word)... but also continuous predictors at the trial level?

Data and code availability

The simulation results as well as the R code to reproduce the simulations are available on GitHub: https://github.com/lnalborczyk/brms_meeg. The **neurogam** R package is available at <https://github.com/lnalborczyk/neurogam>.

Packages

We used R version 4.4.3 (R Core Team, 2025) and the following R packages: assertthat v. 0.2.1 (Wickham, 2019), brms v. 2.22.0 (Bürkner, 2017, 2018, 2021), changepoint v. 2.3 (Killick et al., 2024; Killick & Eckley, 2014), doParallel v. 1.0.17 (Corporation & Weston, 2022), easystats v. 0.7.4 (Lüdtke et al., 2022), foreach v. 1.5.2 (Microsoft & Weston, 2022), furrr v. 0.3.1 (Vaughan & Dancho, 2022), future v. 1.34.0 (Bengtsson, 2021), ggrepel v. 0.9.6 (Slowikowski, 2024), glue v. 1.8.0 (Hester & Bryan, 2024), grateful v. 0.2.11 (Rodriguez-Sanchez & Jackson, 2024), knitr v. 1.50 (Xie, 2014, 2015, 2025), MetBrewer v. 0.2.0 (Mills, 2022), neurogam v. 0.0.1 (Nalborczyk, 2025), pakret v. 0.2.2 (Gallou, 2024), patchwork v. 1.3.0 (T. L. Pedersen, 2024), rmarkdown v. 2.29 (Allaire et al., 2024; Xie et al., 2018, 2020), scales v. 1.3.0 (Wickham et al., 2023), scico v. 1.5.0 (T. L. Pedersen & Crameri, 2023), tidybayes v. 3.0.7 (Kay, 2024), tidytext v. 0.4.2 (Silge & Robinson, 2016), tidyverse v. 2.0.0 (Wickham et al., 2019).

Acknowledgements

Centre de Calcul Intensif d’Aix-Marseille is acknowledged for granting access to its high performance computing resources.

References

- Abugaber, D., Finestrat, I., Luque, A., & Morgan-Short, K. (2023). Generalized additive mixed modeling of EEG supports dual-route accounts of morphosyntax in suggesting no word frequency effects on processing of regular grammatical forms. *Journal of Neurolinguistics*, 67, 101137. <https://doi.org/10.1016/j.jneuroling.2023.101137>
- Allaire, J., Xie, Y., Dervieux, C., McPherson, J., Luraschi, J., Ushey, K., Atkins, A., Wickham, H., Cheng, J., Chang, W., & Iannone, R. (2024). *rmarkdown: Dynamic documents for r*. <https://github.com/rstudio/rmarkdown>
- Baayen, R. H., & Linke, M. (2020). *Generalized Additive Mixed Models* (pp. 563–591). Springer International Publishing. https://doi.org/10.1007/978-3-030-46216-1_23
- Baayen, R. H., Rij, J. van, Cat, C. de, & Wood, S. (2018). *Autocorrelated errors in experimental data in the language sciences: Some solutions offered by generalized additive mixed models* (pp. 49–69). Springer International Publishing. https://doi.org/10.1007/978-3-319-69830-4_4
- Bengtsson, H. (2021). A unifying framework for parallel and distributed processing in r using futures. *The R Journal*, 13(2), 208–227. <https://doi.org/10.32614/RJ-2021-048>
- Benjamini, Y., & Hochberg, Y. (1995). Controlling the False Discovery Rate: A Practical and Powerful Approach to Multiple Testing. *Journal of the Royal Statistical Society Series B: Statistical Methodology*, 57(1), 289–300. <https://doi.org/10.1111/j.2517-6161.1995.tb02031.x>
- Benjamini, Y., & Yekutieli, D. (2001). The control of the false discovery rate in multiple testing under dependency. *The Annals of Statistics*, 29(4). <https://doi.org/10.1214/aos/1013699998>
- Bürkner, P.-C. (2017). brms: An R package for Bayesian multilevel models using Stan. *Journal of Statistical Software*, 80(1), 1–28. <https://doi.org/10.18637/jss.v080.i01>
- Bürkner, P.-C. (2018). Advanced Bayesian multilevel modeling with the R package brms. *The R Journal*, 10(1), 395–411. <https://doi.org/10.32614/RJ-2018-017>
- Bürkner, P.-C. (2021). Bayesian item response modeling in R with brms and Stan. *Journal of Statistical Software*, 100(5), 1–54. <https://doi.org/10.18637/jss.v100.i05>
- Combrisson, E., & Jerbi, K. (2015). Exceeding chance level by chance: The caveat of theoretical chance levels in brain signal classification and statistical assessment of decoding accuracy. *Journal of Neuroscience Methods*, 250, 126–136. <https://doi.org/10.1016/j.jneumeth.2015.01.010>
- Coretta, S., & Bürkner, P.-C. (2025). *Bayesian beta regressions with brms in r: A tutorial for phoneticians*. http://dx.doi.org/10.31219/osf.io/f9rqg_v1
- Corporation, M., & Weston, S. (2022). *doParallel: Foreach parallel adaptor for the “parallel” package*. <https://CRAN.R-project.org/package=doParallel>
- Dimigen, O., & Ehinger, B. V. (2021). Regression-based analysis of combined EEG and eye-tracking data: Theory and applications. *Journal of Vision*, 21(1), 3. <https://doi.org/10.1167/jov.21.1.3>
- Dinga, R., Fraza, C. J., Bayer, J. M. M., Kia, S. M., Beckmann, C. F., & Marquand, A. F. (2021). *Normative modeling of neuroimaging data using generalized additive models of location scale and shape*. <http://dx.doi.org/10.1101/2021.06.14.448106>
- Dunagan, D., Jordan, T., Hale, J. T., Pylkkänen, L., & Chacón, D. A. (2024). *Evaluating the timecourses of morpho-orthographic, lexical, and grammatical processing following rapid parallel visual presentation: An EEG investigation in english*. <http://dx.doi.org/10.1101/2024.04.10.588861>
- Ehinger, B. V., & Dimigen, O. (2019). Unfold: An integrated toolbox for overlap correction, non-linear modeling, and regression-based EEG analysis. *PeerJ*, 7, e7838. <https://doi.org/10.7717/peerj.7838>
- Eklund, A., Nichols, T. E., & Knutsson, H. (2016). Cluster failure: Why fMRI inferences for

- spatial extent have inflated false-positive rates. *Proceedings of the National Academy of Sciences*, 113(28), 7900–7905. <https://doi.org/10.1073/pnas.1602413113>
- Fischer, Adrian G., & Ullsperger, M. (2013). Real and Fictive Outcomes Are Processed Differently but Converge on a Common Adaptive Mechanism. *Neuron*, 79(6), 1243–1255. <https://doi.org/10.1016/j.neuron.2013.07.006>
- Frossard, J., & Renaud, O. (2021). Permutation Tests for Regression, ANOVA, and Comparison of Signals: The **permuco** Package. *Journal of Statistical Software*, 99(15). <https://doi.org/10.18637/jss.v099.i15>
- Frossard, J., & Renaud, O. (2022). The cluster depth tests: Toward point-wise strong control of the family-wise error rate in massively univariate tests with application to M/EEG. *NeuroImage*, 247, 118824. <https://doi.org/10.1016/j.neuroimage.2021.118824>
- Gabry, J., Simpson, D., Vehtari, A., Betancourt, M., & Gelman, A. (2019). Visualization in Bayesian workflow. *Journal of the Royal Statistical Society: Series A (Statistics in Society)*, 182(2), 389–402. <https://doi.org/10.1111/rssa.12378>
- Gallou, A. (2024). *pakret: Cite “R” packages on the fly in “R Markdown” and “Quarto”*. <https://CRAN.R-project.org/package=pakret>
- Gelman, A., Vehtari, A., Simpson, D., Margossian, C. C., Carpenter, B., Yao, Y., Kennedy, L., Gabry, J., Bürkner, P.-C., & Modrák, M. (2020). Bayesian workflow. *arXiv:2011.01808 [Stat]*. <http://arxiv.org/abs/2011.01808>
- Gramfort, A. (2013). MEG and EEG data analysis with MNE-python. *Frontiers in Neuroscience*, 7. <https://doi.org/10.3389/fnins.2013.00267>
- Hastie, T. J., & Tibshirani, R. J. (2017). *Generalized Additive Models*. Routledge. <https://doi.org/10.1201/9780203753781>
- Hauk, O., Davis, M. H., Ford, M., Pulvermüller, F., & Marslen-Wilson, W. D. (2006). The time course of visual word recognition as revealed by linear regression analysis of ERP data. *NeuroImage*, 30(4), 1383–1400. <https://doi.org/10.1016/j.neuroimage.2005.11.048>
- Hayasaka, S. (2003). Validating cluster size inference: Random field and permutation methods. *NeuroImage*, 20(4), 2343–2356. <https://doi.org/10.1016/j.neuroimage.2003.08.003>
- Hendrix, P., Bolger, P., & Baayen, H. (2017). Distinct ERP signatures of word frequency, phrase frequency, and prototypicality in speech production. *Journal of Experimental Psychology: Learning, Memory, and Cognition*, 43(1), 128–149. <https://doi.org/10.1037/a0040332>
- Hester, J., & Bryan, J. (2024). *glue: Interpreted string literals*. <https://CRAN.R-project.org/package=glue>
- Holm, S. (1979). A simple sequentially rejective multiple test procedure. *Scandinavian Journal of Statistics*, 6(2), 65–70. <http://www.jstor.org/stable/4615733>
- Kay, M. (2024). *tidybayes: Tidy data and geoms for Bayesian models*. <https://doi.org/10.5281/zenodo.1308151>
- Killick, R., & Eckley, I. A. (2014). changepoint: An R package for changepoint analysis. *Journal of Statistical Software*, 58(3), 1–19. <https://www.jstatsoft.org/article/view/v058i03>
- Killick, R., Haynes, K., & Eckley, I. A. (2022). *changepoint: An R package for changepoint analysis*. <https://CRAN.R-project.org/package=changepoint>
- Killick, R., Haynes, K., & Eckley, I. A. (2024). *changepoint: An R package for changepoint analysis*. <https://CRAN.R-project.org/package=changepoint>
- King, J.-R., & Dehaene, S. (2014). Characterizing the dynamics of mental representations: the temporal generalization method. *Trends in Cognitive Sciences*, 18(4), 203–210. <https://doi.org/10.1016/j.tics.2014.01.002>
- Kruschke, J. K., & Liddell, T. M. (2017). The Bayesian New Statistics: Hypothesis testing, estimation, meta-analysis, and power analysis from a Bayesian perspective. *Psychonomic Bulletin & Review*, 25(1), 178–206. <https://doi.org/10.3758/s13423-016-1221-4>
- Kryuchkova, T., Tucker, B. V., Wurm, L. H., & Baayen, R. H. (2012). Danger and usefulness are detected early in auditory lexical processing: Evidence from electroencephalography.

- Brain and Language*, 122(2), 81–91. <https://doi.org/10.1016/j.bandl.2012.05.005>
- Luck, S. J., & Gaspelin, N. (2017). How to get statistically significant effects in any ERP experiment (and why you shouldn't). *Psychophysiology*, 54(1), 146–157. <https://doi.org/10.1111/psyp.12639>
- Lüdtke, D., Ben-Shachar, M. S., Patil, I., Wiernik, B. M., Bacher, E., Thériault, R., & Makowski, D. (2022). easystats: Framework for easy statistical modeling, visualization, and reporting. *CRAN*. <https://doi.org/10.32614/CRAN.package.easystats>
- Maris, E. (2011). Statistical testing in electrophysiological studies. *Psychophysiology*, 49(4), 549–565. <https://doi.org/10.1111/j.1469-8986.2011.01320.x>
- Maris, E., & Oostenveld, R. (2007). Nonparametric statistical testing of EEG- and MEG-data. *Journal of Neuroscience Methods*, 164(1), 177–190. <https://doi.org/10.1016/j.jneumeth.2007.03.024>
- Meulman, N., Sprenger, S. A., Schmid, M. S., & Wieling, M. (2023). GAM-based individual difference measures for L2 ERP studies. *Research Methods in Applied Linguistics*, 2(3), 100079. <https://doi.org/10.1016/j.rmal.2023.100079>
- Meulman, N., Wieling, M., Sprenger, S. A., Stowe, L. A., & Schmid, M. S. (2015). Age Effects in L2 Grammar Processing as Revealed by ERPs and How (Not) to Study Them. *PLOS ONE*, 10(12), e0143328. <https://doi.org/10.1371/journal.pone.0143328>
- Microsoft, & Weston, S. (2022). *foreach: Provides foreach looping construct*. <https://CRAN.R-project.org/package=foreach>
- Miller, D. L. (2025). Bayesian views of generalized additive modelling. *Methods in Ecology and Evolution*. <https://doi.org/10.1111/2041-210x.14498>
- Mills, B. R. (2022). *MetBrewer: Color palettes inspired by works at the metropolitan museum of art*. <https://CRAN.R-project.org/package=MetBrewer>
- Nalborczyk, L. (2025). *neurogam: Precise temporal localisation of m/EEG effects with bayesian generalised additive multilevel models*.
- Nalborczyk, L., Batailler, C., Loevenbruck, H., Vilain, A., & Bürkner, P.-C. (2019). An Introduction to Bayesian Multilevel Models Using brms: A Case Study of Gender Effects on Vowel Variability in Standard Indonesian. *Journal of Speech, Language, and Hearing Research*, 62(5), 1225–1242. https://doi.org/10.1044/2018_jslhr-s-18-0006
- Nalborczyk, L., Hauw, F., Torcy, H. de, Dehaene, S., & Cohen, L. (in preparation). *Neural and representational dynamics of tickertape synesthesia*.
- Pedersen, E. J., Miller, D. L., Simpson, G. L., & Ross, N. (2019). Hierarchical generalized additive models in ecology: An introduction with mgcv. *PeerJ*, 7, e6876. <https://doi.org/10.7717/peerj.6876>
- Pedersen, T. L. (2024). *patchwork: The composer of plots*. <https://CRAN.R-project.org/package=patchwork>
- Pedersen, T. L., & Cramer, F. (2023). *scico: Colour palettes based on the scientific colour-maps*. <https://CRAN.R-project.org/package=scico>
- Pernet, C. R. (2022). Electroencephalography robust statistical linear modelling using a single weight per trial. *Aperture Neuro*, 2, 1–22. <https://doi.org/10.52294/apertureneuro.2022.2.seo09435>
- Pernet, C. R., Chauveau, N., Gaspar, C., & Rousselet, G. A. (2011). LIMO EEG: A Toolbox for Hierarchical Linear Modeling of ElectroEncephaloGraphic Data. *Computational Intelligence and Neuroscience*, 2011, 1–11. <https://doi.org/10.1155/2011/831409>
- Pernet, C. R., Latinus, M., Nichols, T. E., & Rousselet, G. A. (2015). Cluster-based computational methods for mass univariate analyses of event-related brain potentials/fields: A simulation study. *Journal of Neuroscience Methods*, 250, 85–93. <https://doi.org/10.1016/j.jneumeth.2014.08.003>
- R Core Team. (2025). *R: A language and environment for statistical computing*. R Foundation for Statistical Computing. <https://www.R-project.org/>

- Rasmussen, C. E., & Williams, C. K. I. (2005). *Gaussian Processes for Machine Learning*.
<https://doi.org/10.7551/mitpress/3206.001.0001>
- Rigby, R. A., & Stasinopoulos, D. M. (2005). Generalized Additive Models for Location, Scale and Shape. *Journal of the Royal Statistical Society Series C: Applied Statistics*, 54(3), 507–554. <https://doi.org/10.1111/j.1467-9876.2005.00510.x>
- Rij, J. van, Hendriks, P., Rijn, H. van, Baayen, R. H., & Wood, S. N. (2019). Analyzing the Time Course of Pupillometric Data. *Trends in Hearing*, 23. <https://doi.org/10.1177/2331216519832483>
- Riutort-Mayol, G., Bürkner, P.-C., Andersen, M. R., Solin, A., & Vehtari, A. (2023). Practical Hilbert space approximate Bayesian Gaussian processes for probabilistic programming. *Statistics and Computing*, 33(1), 17. <https://doi.org/10.1007/s11222-022-10167-2>
- Rodriguez-Sanchez, F., & Jackson, C. P. (2024). *grateful: Facilitate citation of R packages*. <https://pakillo.github.io/grateful/>
- Rosenblatt, J. D., Finos, L., Weeda, W. D., Solari, A., & Goeman, J. J. (2018). All-Resolutions Inference for brain imaging. *NeuroImage*, 181, 786–796. <https://doi.org/10.1016/j.neuroimage.2018.07.060>
- Rousset, G. A. (2025). Using cluster-based permutation tests to estimate MEG/EEG onsets: How bad is it? *European Journal of Neuroscience*, 61(1), e16618. <https://doi.org/10.1111/ejn.16618>
- Rousset, G. A., Pernet, C. R., Bennett, P. J., & Sekuler, A. B. (2008). Parametric study of EEG sensitivity to phase noise during face processing. *BMC Neuroscience*, 9(1). <https://doi.org/10.1186/1471-2202-9-98>
- Sassenhagen, J., & Draschkow, D. (2019). Cluster-based permutation tests of MEG/EEG data do not establish significance of effect latency or location. *Psychophysiology*, 56(6). <https://doi.org/10.1111/psyp.13335>
- Silge, J., & Robinson, D. (2016). tidytext: Text mining and analysis using tidy data principles in r. *JOSS*, 1(3). <https://doi.org/10.21105/joss.00037>
- Skukies, R., & Ehinger, B. (2021). Modelling event duration and overlap during EEG analysis. *Journal of Vision*, 21(9), 2037. <https://doi.org/10.1167/jov.21.9.2037>
- Skukies, R., Schepers, J., & Ehinger, B. (2024, December 9). *Brain responses vary in duration - modeling strategies and challenges*. <https://doi.org/10.1101/2024.12.05.626938>
- Slowikowski, K. (2024). *ggrepel: Automatically position non-overlapping text labels with “ggplot2”*. <https://CRAN.R-project.org/package=ggrepel>
- Smith, N. J., & Kutas, M. (2014a). Regression-based estimation of ERP waveforms: I. The rERP framework. *Psychophysiology*, 52(2), 157–168. <https://doi.org/10.1111/psyp.12317>
- Smith, N. J., & Kutas, M. (2014b). Regression-based estimation of ERP waveforms: II. Non-linear effects, overlap correction, and practical considerations. *Psychophysiology*, 52(2), 169–181. <https://doi.org/10.1111/psyp.12320>
- Smith, S., & Nichols, T. (2009). Threshold-free cluster enhancement: Addressing problems of smoothing, threshold dependence and localisation in cluster inference. *NeuroImage*, 44(1), 83–98. <https://doi.org/10.1016/j.neuroimage.2008.03.061>
- Sóskuthy, M. (2017). *Generalised additive mixed models for dynamic analysis in linguistics: A practical introduction*. <https://doi.org/10.48550/ARXIV.1703.05339>
- Sóskuthy, M. (2021). Evaluating generalised additive mixed modelling strategies for dynamic speech analysis. *Journal of Phonetics*, 84, 101017. <https://doi.org/10.1016/j.wocn.2020.101017>
- Teichmann, L. (2022). An empirically driven guide on using bayes factors for m/EEG decoding. *Aperture Neuro*, 2, 1–10. <https://doi.org/10.52294/apertureneuro.2022.2.maoc6465>
- Tremblay, A., & Newman, A. J. (2014). Modeling nonlinear relationships in ERP data using mixed-effects regression with R examples. *Psychophysiology*, 52(1), 124–139. <https://doi.org/10.1111/psyp.12299>

- Umlauf, N., Klein, N., & Zeileis, A. (2018). BAMLSS: Bayesian Additive Models for Location, Scale, and Shape (and Beyond). *Journal of Computational and Graphical Statistics*, 27(3), 612–627. <https://doi.org/10.1080/10618600.2017.1407325>
- Ushey, K., Allaire, J., & Tang, Y. (2024). *Reticulate: Interface to 'python'*. <https://CRAN.R-project.org/package=reticulate>
- Vaughan, D., & Dancho, M. (2022). *furrr: Apply mapping functions in parallel using futures*. <https://CRAN.R-project.org/package=furrr>
- Wickham, H. (2019). *assertthat: Easy pre and post assertions*. <https://CRAN.R-project.org/package=assertthat>
- Wickham, H., Averick, M., Bryan, J., Chang, W., McGowan, L. D., François, R., Grolemund, G., Hayes, A., Henry, L., Hester, J., Kuhn, M., Pedersen, T. L., Miller, E., Bache, S. M., Müller, K., Ooms, J., Robinson, D., Seidel, D. P., Spinu, V., ... Yutani, H. (2019). Welcome to the tidyverse. *Journal of Open Source Software*, 4(43), 1686. <https://doi.org/10.21105/joss.01686>
- Wickham, H., Pedersen, T. L., & Seidel, D. (2023). *scales: Scale functions for visualization*. <https://CRAN.R-project.org/package=scales>
- Wieling, M. (2018). Analyzing dynamic phonetic data using generalized additive mixed modeling: A tutorial focusing on articulatory differences between L1 and L2 speakers of English. *Journal of Phonetics*, 70, 86–116. <https://doi.org/10.1016/j.wocn.2018.03.002>
- Winter, B., & Wieling, M. (2016). How to analyze linguistic change using mixed models, Growth Curve Analysis and Generalized Additive Modeling. *Journal of Language Evolution*, 1(1), 7–18. <https://doi.org/10.1093/jole/lzv003>
- Wood, S. N. (2003). Thin Plate Regression Splines. *Journal of the Royal Statistical Society Series B: Statistical Methodology*, 65(1), 95–114. <https://doi.org/10.1111/1467-9868.00374>
- Wood, S. N. (2017a). *Generalized Additive Models*. Chapman; Hall/CRC. <https://doi.org/10.1201/9781315370279>
- Wood, S. N. (2017b). *Generalized additive models: An introduction with r* (2nd ed.). Chapman; Hall/CRC.
- Wüllhorst, V., Wüllhorst, R., Overmeyer, R., & Endrass, T. (2025). Comprehensive Analysis of Event-Related Potentials of Response Inhibition: The Role of Negative Urgency and Compulsivity. *Psychophysiology*, 62(2). <https://doi.org/10.1111/psyp.70000>
- Xie, Y. (2014). knitr: A comprehensive tool for reproducible research in R. In V. Stodden, F. Leisch, & R. D. Peng (Eds.), *Implementing reproducible computational research*. Chapman; Hall/CRC.
- Xie, Y. (2015). *Dynamic documents with R and knitr* (2nd ed.). Chapman; Hall/CRC. <https://yihui.org/knitr/>
- Xie, Y. (2025). *knitr: A general-purpose package for dynamic report generation in R*. <https://yihui.org/knitr/>
- Xie, Y., Allaire, J. J., & Grolemund, G. (2018). *R markdown: The definitive guide*. Chapman; Hall/CRC. <https://bookdown.org/yihui/rmarkdown>
- Xie, Y., Dervieux, C., & Riederer, E. (2020). *R markdown cookbook*. Chapman; Hall/CRC. <https://bookdown.org/yihui/rmarkdown-cookbook>
- Yeung, N., Bogacz, R., Holroyd, C. B., & Cohen, J. D. (2004). Detection of synchronized oscillations in the electroencephalogram: An evaluation of methods. *Psychophysiology*, 41(6), 822–832. <https://doi.org/10.1111/j.1469-8986.2004.00239.x>

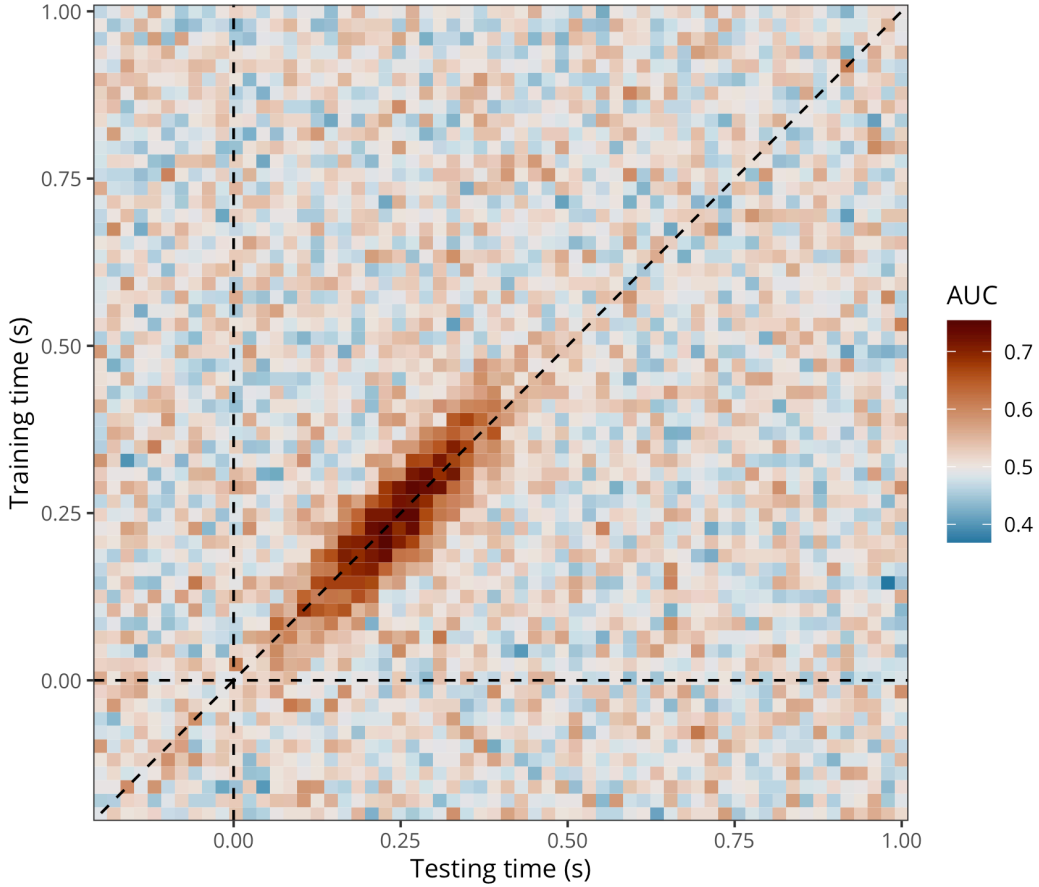
Appendix A

Application to 2D time-resolved decoding results (cross-temporal generalisation)

Assume we have M/EEG data and we have conducted cross-temporal generalisation analyses (King & Dehaene, 2014). As a result, we have a 2D matrix where each element contains the decoding accuracy (e.g., ROC AUC) of a classifier trained at timestep train_i and tested at timestep test_j (Figure A1).

Figure A1

Exemplary (simulated) group-level average cross-temporal generalisation matrix of decoding performance (ROC AUC).



To model cross-temporal generalisation matrices of decoding performance (ROC AUC), we extended the initial (decoding) GAM to take into account the bivariate temporal distribution of AUC values, thus producing naturally smoothed estimates (timecourses) of AUC values and posterior probabilities. This model can be written as follows:

$$\begin{aligned} \text{AUC}_i &\sim \text{Beta}(\mu_i, \phi) \\ g(\mu_i) &= f(\text{train}_i, \text{test}_i) \end{aligned}$$

where we assume that AUC values come from a Beta distribution with two parameters μ and ϕ . We can think of $f(\text{train}_i, \text{test}_i)$ as a surface (a smooth function of two variables) that we can model using a 2-dimensional splines. Let $\mathbf{s}_i = (\text{train}_i, \text{test}_i)$ be some pair of training and testing samples, and let $\mathbf{k}_m = (\text{train}_m, \text{test}_m)$ denote the m^{th} knot in the domain of train_i and test_i . We can then express the smooth function as:

$$f(\text{train}_i, \text{test}_i) = \alpha + \sum_{m=1}^M \beta_m b_m(\tilde{s}_i, \tilde{k}_m)$$

508 Note that $b_m(\cdot)$ is a basis function that maps $R \times R \rightarrow R$. A popular bivariate basis
 509 function uses *thin-plate splines* (Wood, 2003), which extend to $\mathbf{s}_i \in \mathbb{R}^d$ and ∂l_g penalties. These
 510 splines are designed to interpolate and approximate smooth surfaces over two dimensions (hence
 511 the “bivariate” term). For $d = 2$ dimensions and $l = 2$ (smoothness penalty involving second
 512 order derivative):

$$f(\tilde{s}_i) = \alpha + \beta_1 x_i + \beta_2 z_i + \sum_{m=1}^M \beta_{2+m} b_m(\tilde{s}_i, \tilde{k}_m)$$

513 using the the radial basis function given by:

$$b_m(\tilde{s}_i, \tilde{k}_m) = \left\| \tilde{s}_i - \tilde{k}_m \right\|^2 \log \left\| \tilde{s}_i - \tilde{k}_m \right\|$$

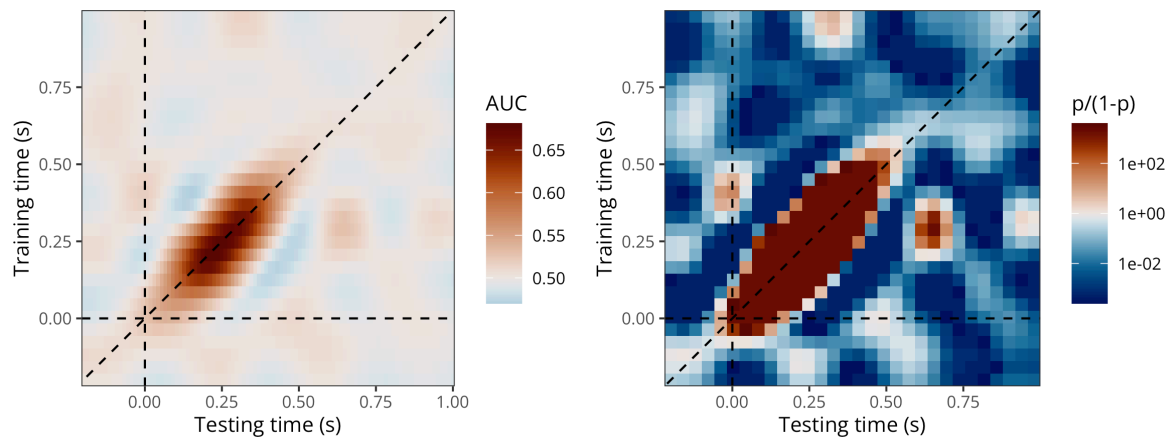
514 where $\|\mathbf{s}_i - \mathbf{k}_m\|$ is the Euclidean distance between the covariate \mathbf{s}_i and the knot location
 515 \mathbf{k}_m . We fitted this model using **brms**...

```
# fitting a GAM with two temporal dimensions
timegen_gam <- brm(
  # 2D thin-plate spline (tp)
  auc ~ t2(train_time, test_time, bs = "tp", k = 20),
  data = timegen_data,
  family = Beta(),
  warmup = 1000,
  iter = 2000,
  chains = 8,
  cores = 8,
  file = "models/timegen_gam_t2.rds"
)

# fitting a GP with two temporal dimensions
# timegen_gp <- brm(
#   auc ~ gp(train_time, test_time, k = 20),
#   data = timegen_data,
#   family = Beta(),
#   control = list(adapt_delta = 0.95),
#   iter = 2000,
#   chains = 4,
#   cores = 4,
#   file = "models/timegen_gp.rds"
# )
```

Figure A2

Predicted AUC values (left) and posterior probabilities of decoding accuracy being above chance level (right) according to the bivariate GAM.



516 Could be extended to spatial and temporal dimensions with formulas such as `te(x, y,`
 517 `Time, d = c(2, 1))...`

Appendix B

Alternative to GAMs: Approximate Gaussian Process regression

A Gaussian process (GP) is a stochastic process that defines the distribution over a collection of random variables indexed by a continuous variable, that is $\{f(t) : t \in \mathcal{T}\}$ for some index set \mathcal{T} (Rasmussen & Williams, 2005; Riutort-Mayol et al., 2023). Whereas Bayesian linear regression outputs a distribution over the parameters of some predefined parametric model, the GP approach, in contrast, is a non-parametric approach, in that it finds a distribution over the possible functions that are consistent with the observed data. However, note that nonparametric does not mean there aren't parameters, it means that there are infinitely many parameters.

From [brms documentation](#): A GP is a stochastic process, which describes the relation between one or more predictors $x = (x_1, \dots, x_d)$ and a response $f(x)$, where d is the number of predictors. A GP is the generalization of the multivariate normal distribution to an infinite number of dimensions. Thus, it can be interpreted as a prior over functions. The values of $f()$ at any finite set of locations are jointly multivariate normal, with a covariance matrix defined by the covariance kernel $k_p(x_i, x_j)$, where p is the vector of parameters of the GP:

$$(f(x_1), \dots, f(x_n)) \sim \text{MVN}\left(0, (k_p(x_i, x_j))_{i,j=1}^n\right)$$

The smoothness and general behaviour of the function f depends only on the choice of covariance kernel, which ensures that values that are close together in the input space will be mapped to similar output values...

From this perspective, f is a realisation of an infinite dimensional normal distribution:

$$f \sim \text{Normal}(0, C(\lambda))$$

where C is a covariance kernel with hyperparameters λ that defines the covariance between two function values $f(t_1)$ and $f(t_2)$ for two time points t_1 and t_2 (Rasmussen & Williams, 2005). Similar to the different choices of the basis function for splines, different choices of the covariance kernel lead to different GPs. In this article, we consider the squared-exponential (a.k.a. radial basis function) kernel, which computes the squared distance between points and converts it into a measure of similarity. It is defined as:

$$C(\lambda) := C(t_1, t_2, \sigma, \gamma) := \sigma^2 \exp\left(-\frac{\|t_1 - t_2\|^2}{2\gamma^2}\right)$$

with hyperparameters $\lambda = (\sigma, \gamma)$, expressing the overall scale of GP and the length-scale, respectively (Rasmussen & Williams, 2005). The advantages of this kernel are that it is computationally efficient and (infinitely) smooth making it a reasonable choice for the purposes of the present article. Here again, λ hyperparameters are estimated from the data, along with all other model parameters.

Taken from <https://michael-franke.github.io/Bayesian-Regression/practice-sheets/10c-Gaussian-processes.html>: For a given vector \mathbf{x} , we can use the kernel to construct finite multi-variate normal distribution associated with it like so:

$$\mathbf{x} \mapsto_{GP} \text{MVNormal}(m(\mathbf{x}), k(\mathbf{x}, \mathbf{x}))$$

where m is a function that specifies the mean for the distribution associated with \mathbf{x} . This mapping is essentially the Gaussian process: a systematic association of vectors of arbitrary length with a suitable multi-variate normal distribution.

Low-rank approximate Gaussian processes are of main interest in machine learning and statistics due to the high computational demands of exact Gaussian process models (Riutort-Mayol et al., 2023)...

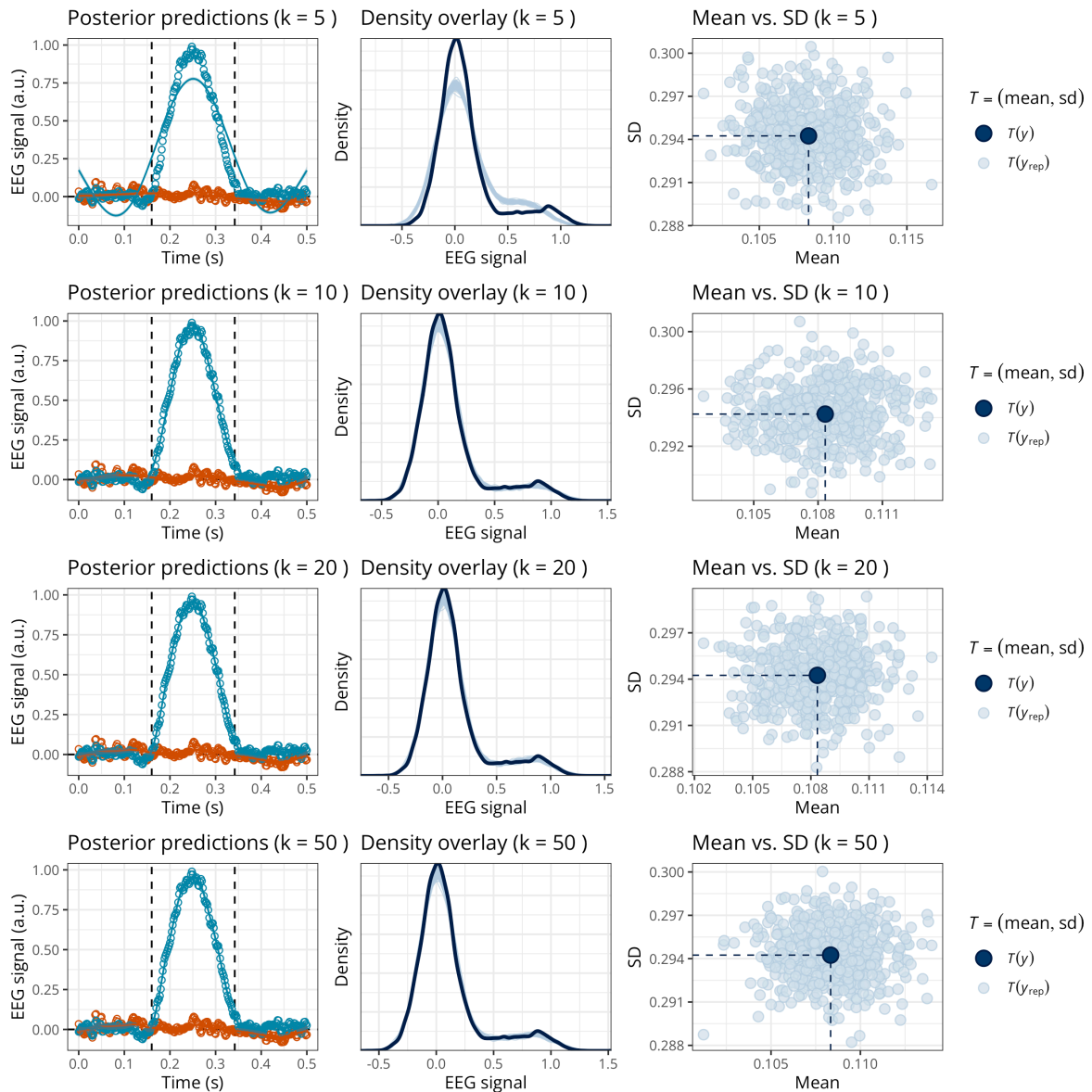
Appendix C

How to choose the GAM basis dimension?

Here provide recommendation about how to define k . An option is to vary k and examine the predictions and posterior predictive checks (PPCs) of each model... In this example (Figure C1)... However, it is not possible to provide general recommendations, as the optimal k depends on the sampling rate, the preprocessing steps (e.g., signal-to-noise ratio, low-pass filtering, etc), and the neural dynamics of the phenomenon under study.

Figure C1

Posterior predictions and posterior predictive checks for the GAM with varying k (in rows).



Appendix D

Integration with MNE-Python

For users who are already familiar with **brms**, the recommended pipeline is to import ERPs or decoding results in R and analyse these data using the code provided in the main paper. However, it is also possible to simply call functions from the **neurogam** R package (available at <https://github.com/ljalborczyk/neurogam>), which come with sensible defaults.

```
# installing (if needed) and loading the neurogam R package
# remotes::install_github("https://github.com/ljalborczyk/neurogam")
library(neurogam)

# using the testing_through_time() function from the neurogam package
gam_onset_offset <- testing_through_time(
  data = raw_df,
  threshold = 10,
  participant_id = "participant", meeg_id = "eeg",
  time_id = "time", predictor_id = "condition",
  warmup = 1000, iter = 5000, chains = 4, cores = 4
)

# displaying the results
gam_onset_offset$clusters
```

The **neurogam** package can also be called from Python using the **rpy2** module, and can easily be integrated into MNE-Python pipelines. For example, we use it below to estimate the onset and offset of effects for one channel from a MNE evoked object. Note that the code used to reshape the **sample** MNE dataset is provided later, and we refer to the [MNE documentation](#) about converting MNE epochs to **Pandas** dataframes in long format.

```
# loading the Python modules
import rpy2.objects as robjects
from rpy2.objects.packages import importr
from rpy2.objects import pandas2ri
from rpy2.objects.conversion import localconverter

# importing the "neurogam" R package
neurogam = importr("neurogam")

# activating automatic pandas-R conversion
pandas2ri.activate()

# assuming reshaped_df is some M/EEG data reshaped in long format
with localconverter(robjects.default_converter + pandas2ri.converter):

    reshaped_df_r = robjects.conversion.py2rpy(reshaped_df)

# using the testing_through_time() function from the neurogam R package
gam_onset_offset = neurogam.testing_through_time(
    data=reshaped_df_r,
    threshold=10,
    multilevel=False
```

```

    )

# displaying the results
print(list(gam_onset_offset) )

# loading the Python modules
import mne
from mne.datasets import sample
import numpy as np
import pandas as pd

# defining the path to the "sample" dataset
path = sample.data_path()

# loading the evoked data
evoked = mne.read_evoked(path / "MEG" / "sample" / "sample_audvis-ave.fif")

# defining a function to reshape the data
def reshape_eeg_channels_as_participants(evoked, condition_labels):

    all_dfs = []

    for evoked, condition in zip(evoked, condition_labels):

        # selecting only EEG channels
        picks = mne.pick_types(evoked.info, meg=False, eeg=True)
        data = evoked.data[picks, :]
        channel_names = np.array(evoked.ch_names)[picks]

        n_channels, n_times = data.shape
        # repeating time for each channel
        times = np.tile(evoked.times, n_channels)
        meeg_values = data.flatten()
        pseudo_participant_ids = np.repeat(channel_names, n_times)

        # converting to dataframe
        df = pd.DataFrame({
            "participant": pseudo_participant_ids,
            "time": times,
            "eeg": meeg_values,
            "condition": condition
        })

        all_dfs.append(df)

    return pd.concat(all_dfs, ignore_index=True)

# picking two evoked conditions
faces = evoked[0]
scrambled = evoked[1]

```

```
# reshaping data by pretending each EEG channel is a participant
reshaped_df = reshape_eeg_channels_as_participants(
    evoked=[faces, scrambled],
    condition_labels=["faces", "scrambled"]
)
```